Applied Surface Science 606 (2022) 154933

Contents lists available at ScienceDirect

Applied Surface Science

journal homepage: www.elsevier.com/locate/apsusc

Full Length Article

Poly(hydroxybutyrate-*co*-hydroxyvalerate) as a biodegradable binder in a negative electrode material for lithium-ion batteries

Andrzej P. Nowak [a,c,*], Konrad Trzciński [a,c], Zuzanna Zarach [a], Jinjin Li [b], Daria Roda [a], Mariusz Szkoda [a,c]

[a] Gdańsk University of Technology, ul. Narutowicza 11/12, 80-233 Gdańsk, Poland
[b] Shanghai Jiao Tong University, 800 Dong Chuan Road, 200240 Shanghai, China
[c] Advanced Materials Center, Gdańsk University of Technology, ul. Narutowicza 11/12, Gdańsk 80-233, Poland

ARTICLE INFO

Keywords:
Binder
Polyhydoxyalkanoates
Lithium-ion battery
Graphite

ABSTRACT

In this work, graphite-based negative electrode for lithium-ion battery consisting a novel and biodegradable binder poly(hydroxybutyrate-*co*-hydroxyvalerate) (PHBV) is compared with standard graphite electrode with polyvinylidene fluoride (PVDF) as a binder. The rate and cycling performance of lithium ion insertion/extraction of electrodes with PHBV in a half-cell configuration are evaluated. Moreover, on the basis of the electrochemical tests it is concluded that the electrode with PHBV binder is characterized by similar specific capacity and diffusion coefficient of lithium ions as conventional graphite electrode with PVDF binder.

1. Introduction

Over the last decades, the rapid expansion of energy storage technologies has been observed, which is mainly due to the ever-increasing demand for small portable devices i.e. mobile phones, laptops, tablets, power banks, and recently, electric vehicles. The most commonly used power sources for those systems are lithium-ion batteries (LIBs). Nowadays, the LIBs market is driven by the automotive industry, with the consequent need to improve the energy density and the life cycle of energy storage systems for future vehicle applications [1]. Therefore, it is still a major challenge to obtain components that will enhance the performance of lithium-ion batteries.

A typical battery consists of a cathode, anode, separator and electrolyte. Both electrodes are manufactured by mixing an active material with a conductive additive and a binder. Binders utilized in LIBs are usually made of synthetic polymers and they are known to affect ageing, coulombic efficiency as well as irreversible capacity loss of a cell [2]. On the one hand, a binder helps to disperse active material and conductive additive in the solvent during the electrode fabrication. Secondly, the role of the binder is to interconnect the slurry components and the current collector together to ensure the mechanical integrity of the electrode. It also acts as an interface between the electrode and electrolyte protecting the electrode from corrosion or the electrolyte from depletion while charge transport through the electrode/electrolyte interface occurs [3]. Moreover, binder determines the rheological profile of the electrode slurry and is expected to exhibit chemical inactivity with lithium ions and electrochemical stability in the studied potential range.

There are many binders that are used in lithium-ion battery cells i.e. polyvinylidene fluoride (PVDF), polytetrafluoroethylene (PTFE), styrene-butadiene rubber (SBR), xanthan gum, carboxymethyl cellulose (CMC), polyvinyl chloride (PVC), polyvinyl alcohol (PVA) and polyacrylic acid (PAA) [4–8]. Depending on the binder used, different effects on the battery performance may be observed, with particular emphasis on the charge–discharge cycling stability [9]. In commercial batteries, the binder that is most commonly used is PVDF, mainly due to its electrochemical, thermal, and mechanical stability, but also thanks to ensuring an excellent adhesion between the electrode film and current collector [10]. PVDF is suitable as a binder for both negative and positive electrodes due to its electrochemical stability between 0 and 5 V [11]. Additionally, the high molecular weight of PVDF makes it convenient for easy manufacturing process, which was also observed for PAA [12]. However, in the presence of lithium salts, after some time, PVDF may suffer from the properties change leading to LiF formation [13]. This salt contributes to cell degradation during cycling. Moreover, lithium intercalated into graphite may react with PVDF and may cause additional heat formation leading to dangerous thermal runaway reactions [14]. Last but not least, PVDF must be in a liquid form to bind

* Corresponding author.
E-mail address: andnowak@pg.edu.pl (A.P. Nowak).

https://doi.org/10.1016/j.apsusc.2022.154933
Received 28 June 2022; Received in revised form 7 September 2022; Accepted 13 September 2022
Available online 17 September 2022
0169-4332/© 2022 The Authors. Published by Elsevier B.V. This is an open access article under the CC BY-NC license (http://creativecommons.org/licenses/by-nc/4.0/).

active material with conducting material and to attach such slurry to a current collector. In a practical approach, an organic solvent, N-methyl-2-pyrrolidone (NMP), is utilized as PVDF is not soluble in water [15]. There are also issues with PVDF/NMP system related to the battery recycling process. Usually, PVDF is removed via dissolution in toxic solvents i.e. NMP or N,N-dimethylformamide (DMF). One may use other, more environmentally friendly solvents, i.e. dihydrolevoglucosenone (Cyrene) or triethyl phosphate (TEP), however poor solubility of PVDF requires an enormous amount of these solvents. The other way to remove PVDF is the pyrolysis process. Unfortunately, it leads to the evolution of hazardous HF which is a very aggressive corrosive agent and requires further gas treatment. From economic point of view, PVDF is relatively more expensive in comparison with natural derived binders [16]. Moreover, natural binders are known to lower the irreversible capacity loss in the first cycle and increase rate performance [17]. The general disadvantage of using plastic binders is that during battery utilization the degradation of the binder may lead to microplastics release that detrimentally affects the environment [18]. As a result, the demand for an ecological binder of natural origin, which can be biodegradable, is still growing. Recently, bio-based plastics attract considerable attention as they exhibit lower impact on waste generation. Among many biodegradable polymers, polyhydroxyalkanoates (PHAs) are considered to be able to replace synthetic polymers, especially in the petrochemical industry [19].

One of the copolymer of polyhydroxyalkanoates, named poly (hydroxybutyrate-*co*-hydroxyvalerate) (PHBV) (see Fig. 1.), is a polyester belonging to PHAs family that is biosynthesized from different types of microorganisms [20]. The PHBV is a thermoplastic, biodegradable, compostable and biocompatible polymer obtained from renewable sources, that is utilized in biomedical [21] and pharmaceutical applications [22].

Due to its biodegradability in water [23], PHBV could be considered as a PVDF replacement in electrode manufacturing. It is estimated that switching from NMP to water in electrode processing could save up to 10.5 % on the pack production cost for LIBs [15].

To the best of our knowledge there are no works related to the utilization of PHBV in energy storage application. It is for the first time when PHBV is proposed as a binder for negative electrode for lithium-ion batteries. We assume that the presence of oxygen atoms in the PHBV structure may affect the chemical composition of solid electrolyte interphase (SEI), and thus prevent LiF formation as it is observed for PVDF based electrode materials [24].

In this work, an investigation on the use of environmentally friendly, biodegradable and low-cost binder PHBV (up to 2$/lb [25]) as an alternative binding material for composite negative electrode with commercial graphite as an active material is presented. For comparison, PVDF ($6.7/lb [26]) was used as a reference binder. Scanning electron microscopy (SEM) was applied in order to examine the solid electrolyte interphase formation process for cycled and non-cycled electrode materials. Cyclic voltammetry and galvanostatic charge/discharge cycles were performed to study an influence of binder on the electrochemical performance of the tested electrode materials The most crucial phenomenon responsible for the charge storage mechanism is based on the intercalation of Li^+ ions to the active material structure, thus the diffusion coefficients were investigated for both types of electrodes.

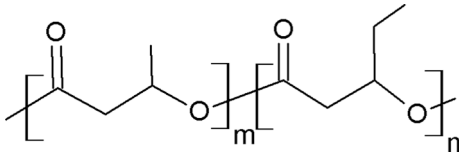

Fig. 1. The chemical structure of poly(hydroxybutyrate-*co*-hydroxyvalerate).

2. Materials and methods

The morphology of the electrode materials before and after electrochemical measurements was investigated using scanning electron microscopy (FEI QUANTA FEG 250) (Quanta 3D FEG, Fei Company), equipped with secondary electron detector in the high vacuum mode (pressure 10^{-4} Pa).

The Raman spectra were recorded using a confocal micro-Raman spectrometer (InVia, Renishaw) with sample excitation, by means of an argon ion laser emitting at 514 nm.

The electrode material, which was coated on a Cu current collector (Schlenk Metallfolien, Germany), was prepared from the slurry containing graphite (80 wt%) (Timrex SFG6, Timcal, Switzerland) the conductive additive (10 wt%) (Carbon Black Super P®, Timcal ltd., Switzerland) and the binder: PHBV (10 wt%) (NaturePlast, PHI002, France) or PVDF (10 wt%) (Solef 6020, Germany) in an appropriate solvent. It was CH_3COOH (99.5 – 99.9 % p.a., POCH, Poland) for PHBV and NMP (99+%, AlfaAesar, USA) for PVDF. Next, the slurry was homogenised for 1 h using ball mill (MM200, Retsch GmbH, Germany). After that, the tape casting material was dried at room temperature, cut from the tape followed by drying under a dynamic vacuum in an oven (Glass Oven B-585 Büchi, Germany) for 24 h at 90 °C. The average mass of the electrode with a diameter of 10 mm was ~ 3 mg with the thickness of 50 μm. Electrode materials are labeled as Timrex_PHBV and Timrex_PVDF.

The electrochemical tests were performed in a two-electrode pouch cell using the electrode material described above as a working electrode, and lithium foil (AlfaAesar, USA) was used as both a counter and a reference electrode. The electrolyte solution was 1 M $LiPF_6$ in EC:DMC ratio 1:1 (LP30 Merck, Germany), and glass fibre (Schleicher&Schüll, Germany) was used as the separator. The cyclic voltammetry and charge/discharge performance experiments were performed on galvanostat/potentiostat (ATLAS 1361 MPG&T, Gdańsk, Poland) within the potential range from 0.005 V to 2 V versus Li/Li^+. The galvanostatic test at a current density of 360 mA/g was done in the potential range from 0.005 V to 3.0 V versus Li/Li^+. The galvanostatic intermittent titration technique (GITT) was performed with the current pulse of 36 mA/g for a duration of 30 min, followed by an open circuit voltage period of 2 h.

The meaning “before” is for the electrode material that was not galvanostatically treated. The meaning “after” refers to the electrode material that was galvanostatically polarized.

3. Results and discussion

Fig. 2 shows cyclic voltammetry curves of TIMREX_PHBV and TMIREX_PVDF electrode materials obtained at different sweep rates applied during measurements.

One may see that the shape of the cv curve for both TRIMEX_PHBV and TRIMEX_PVDF electrode materials is rather similar and in each case, the presence of three redox couple activities, attributed to the changing phase composition generated during lithium intercalation into the graphite structure [27], see Fig. 2c. Five regions, related to the formation of different lithium-graphite intercalation stage compounds, can be distinguished [28]:

$$\text{region 5 (VIII to IV stage)}: \quad LiC_{72} + Li = 2LiC_{36} \tag{1}$$

$$\text{region 4 (IV to III stage)} \quad 3LiC_{36} + Li = 4LiC_{27} \tag{2}$$

$$\text{region 3 (III to II stage)} \quad 2LiC_{27} + Li = 3LiC_{18} \tag{3}$$

$$\text{region 2 (II to II stage)} \quad 2LiC_{18} + Li = 3LiC_{12} \tag{4}$$

$$\text{region 1 (II to I stage)} \quad LiC_{12} + Li = 2LiC_6 \tag{5}$$

These regions are well distinguished for the TIMREX graphite electrode material with both PVDF and PHBV binders. There are some minor

MOST WIEDZY Downloaded from mostwiedzy.pl

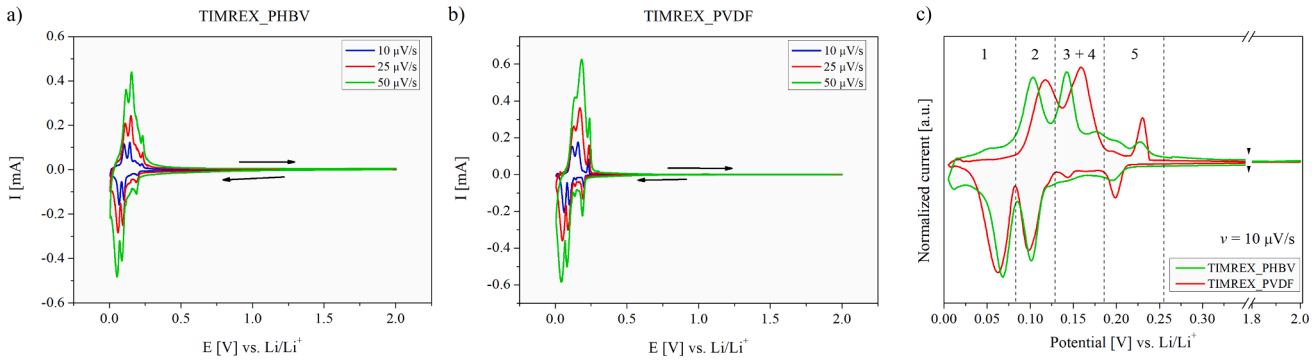

Fig. 2. Cyclic voltammetry curves obtained at different sweep rates for graphite-based negative electrode material with a) PHBV binder, b) PVDF binder and c) direct comparison of curves for PHBV and PVDF binders at $\nu = 10$ μV/s.

shifts in the position of anodic current maxima in regions 2, 3 and 4, however, they might be neglected as they do not affect the electrochemical performance of the electrode materials. We assumed that the origin of current peaks shifted positions is attributed to the type of binder utilized in the electrode manufacturing. Nevertheless, both electrode materials exhibit cathodic and anodic current maxima that are related to lithium-ion intercalation/deintercalation into/from graphite active material. One may also see that the shape of the cv curves for both electrode materials is preserved while different sweep rates were applied, see Fig. 2a and 2b. Moreover, within the studied potential range, no current increase related to PHBV decomposition under oxidation nor reduction is observed. Thus, it may be concluded that PHBV seems to be an appropriate binder for negative electrode material.

In order to investigate the cyclability of the PHBV-based electrode material, charge–discharge measurements at different current densities were performed, see Fig. 3 and Fig. S1. The most evident changes are visible for the first 10 cycles at $j = 36$ mA/g. There is a continuous decrease in specific capacity for anodes consisted of PHBV and PVDF binders, showing the final value of 341 mAh/g for the former and 347 mAh/g for the latter. The calculated capacity fade after the 10 cycles at 36 mA/g is 6.3 % and 5.8 % for PHBV and PVDF, respectively. The results indicate that both binders affect the electrochemical performance of the electrode similarly. A slight difference in the capacity fade value might be due to the electrode manufacturing process. Furthermore, when a current density of 360 mA/g was applied, both materials exhibited specific capacities of very similar values of around 317 mAh/g with capacity retention of 97.9 % after the 20th cycle. However, in each case there is a specific capacity decrease in the first 3 cycles, followed by an increase in the next 4 cycles, and a continuous decrease is observed

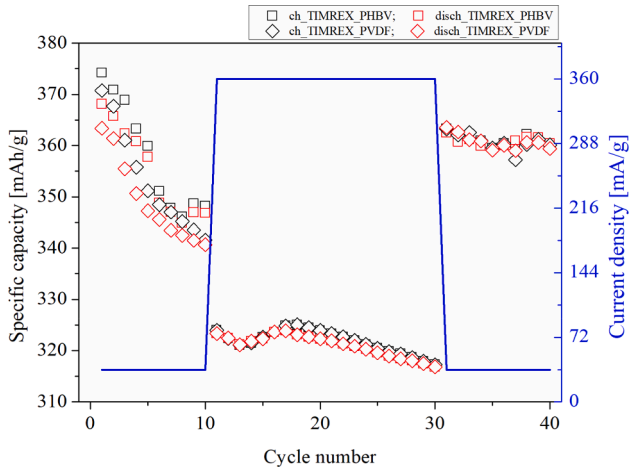

Fig. 3. The charge/discharge cycle performance of graphite electrodes with PHBV (black) or PVDF (red) binders at different current densities.

eventually, up to the 20th cycle. Nevertheless, both materials are characterized by a similar specific capacity value, regardless of the binder type. However, the shape of the curve is not so simple. Moreover, both electrode materials show that the specific capacity of TIMREX_PHBV and TIMRES_PVDF are very close to each other. The analogous effect on both electrode materials can be observed when the current density of 36 mA/g is reapplied, i.e. an increase in the specific capacity to 360 mAh/g, with the capacity fade of only 0.94 % after the 10th cycle. It evidences that PHBV might replace PVDF as a binder in the negative electrode for LIBs, as both electrode materials exhibits similar electrochemical performance. This similarity may suggest that the binding mechanism of PHBV with both electrode components and current collector is similar to what is observed for PVDF. The adhesion strength of PVDF/Cu is greater than that of the PVDF/graphite, and as a result, the loss of electric contact between the electrode component and the current collector appears during very long charge/discharge cycles [29]. However, one should take into account that for lithium iron phosphate (LFP) as the active material and Al as the current collector, the binding interactions between LFP and PVDF are much stronger than that between PVDF and Al [30]. Thus, a more detailed investigation regarding the binding mechanism of PHBV with negative electrode should be performed.

The drastic change in capacity was observed when higher rates (4C, 10C) were applied exhibiting discharge capacity of 210 mAh/g for 4C and 115 mA/g for 10C, see Fig. S1. When cycling back to the initial C/20 rate, the PHBV-based electrode recovered over 90 % of the original discharge capacity at this rate. Extended cycling at a 4C rate led to a huge decrease in capacity from 342 mAh/g for the first discharge to 151 mAh/g for the last, see Fig S2. It gave capacity retention of 44 % suggesting that the PHBV binder is not suitable for high-current applications. It is noteworthy that also for PVDF-based electrodes low discharge capacities are measured at higher rates (2C) [31]. Thus, the decrease in capacity at higher rates is very likely due to the lithium ion transport limitations within graphite electrode.

To determine the influence of PHBV binder on the electrochemical stability of the electrode material, the charge/discharge measurements at current density of 36 mA/g of the TIMREX_PHBV electrode was performed, see Fig. 4. The specific capacity of TIMREX_PHBV electrode material was 357 mAh/g after 100 cycles. It evidences that PHBV-based electrode material is stable during electrochemical measurements, as it was already confirmed by the previous experiment, see Fig. 2. Furthermore, neither a significant capacity loss nor a considerable capacity fade was observed for the PHBV-based electrode. The capacity loss for the extended cycles was 3.43 mAh/g, with the capacity retention of 99.1 % after the 100th cycle. On the basis of the presented results, it may be concluded that the PHBV binder is resistant to dissolution or decomposition in the electrolyte consisting of ethylene carbonate and dimethyl carbonate solvents.

Fig. 5. shows SEM images of the TIMREX_PHBV and TIMREX_PVDF

MOST WIEDZY Downloaded from mostwiedzy.pl

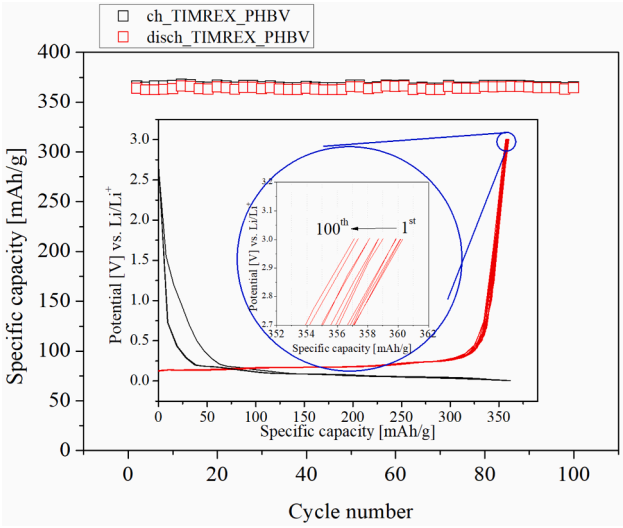

Fig. 4. The cycle performance of TIMREX_PHBV electrode material at $j = 36$ mA/g. Inset: the voltage profile vs capacity.

electrode material before (a,c) and after (b,d) electrochemical measurements, respectively. The surface area of the both electrodes is uniformly covered with a binder network. In the high magnification image, the binders may be distinguished as a sponge-like structure, see inset in Fig. 5a and Fig. 5c. This structure is changed for both electrode materials after galvanostatic charging/discharging, see Fig. 5b and Fig. 5d. The binders seemed to have a more dense structure after electrochemical measurements. However, the presence of the binder structure in the cycled electrode material in Fig. 5b evidences that PHBV was not dissolved by the electrolyte. It also confirms that PHBV is electrochemically stable within the applied potential range. On the other hand, the electrode surface in Fig. 5b and 5d is smoother in comparison with the image in Fig. 5a and 5c, respectively. The smoothness of the surface might be attributed to the formation of the solid electrolyte interface (SEI) [32]. The SEI layer is known to be formed on the graphite electrode's surface in the first reduction cycle, protecting the anode from the direct contact with the electrolyte leading to its dissolution followed by the electrode's destruction [33]. The SEI is an ionic conductor consisting of compounds containing lithium ions. The indirect proof of SEI formation can be seen in the form of bright areas at the edges of the graphite as well as the presence of bright elements of rectangular shape, see the inset in Fig. 5b and 5d. On SEM images the presence of non-electronic conductor parts are usually brighter. It is because a static surface charge is built up on non-conductive samples [34]. Thus, the presence of such bright areas may confirm the formation of the SEI layer.

Fig. 6 shows Raman spectra of TIMREX_PHBV (a) and TIMREX_PVDF (b) electrode materials. The common feature of both materials is the presence of maxima at 1351 cm^{-1}, 1580 cm^{-1} and 2710 cm^{-1}. These maxima are attributed to the presence of carbon atoms of sp^2 hybridization and are named the D band, the G band, and the 2D band, respectively [35]. The D band origins from the breathing motion of the sp^2-ring, while the G maximum is attributed to an in-plane bond stretching vibrations of sp^2 carbon atoms [36]. The 2D band is attributed to the first overtone of the D band [37]. The Raman spectrum of TIMREX_PHBV exhibits also peaks at 842 cm^{-1}, 1720 cm^{-1} and three maxima in the spectral region from 2900 cm^{-1} to 3100 cm^{-1}. The first Raman band originates from C—C vibrational modes in C—COO group, while the second maximum is attributed to the vibrational C═O domain [38]. The bands at 2930 cm^{-1}, 2968 cm^{-1} and 3000 cm^{-1} are assigned to the vibrational mode of C—H bond from methyl, methylene and methyne groups, respectively. The main difference in the Raman spectrum between PHBV and TIMREX_PHBV is the lower intensity of the band ascribed to the methyl group at 2930 cm^{-1}. The difference may be

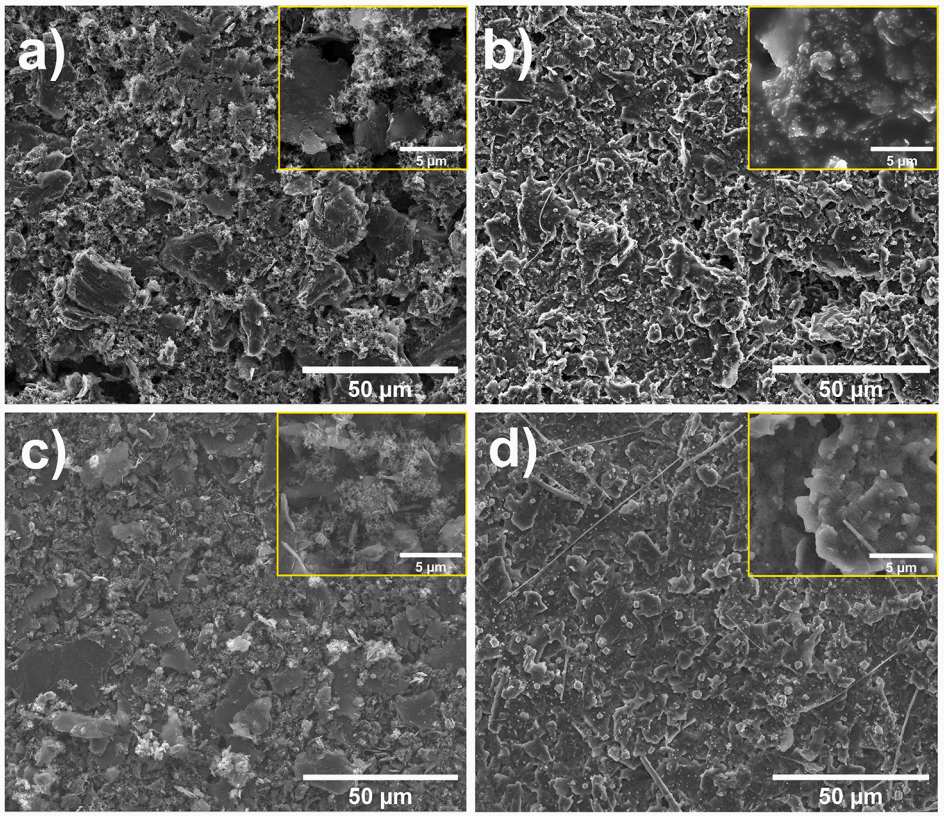

Fig. 5. SEM images of TIMREX_PHBV and TIMREX_PVDF electrode material before (a,c) and after (b,d) electrochemical tests, respectively.

MOST WIEDZY Downloaded from mostwiedzy.pl

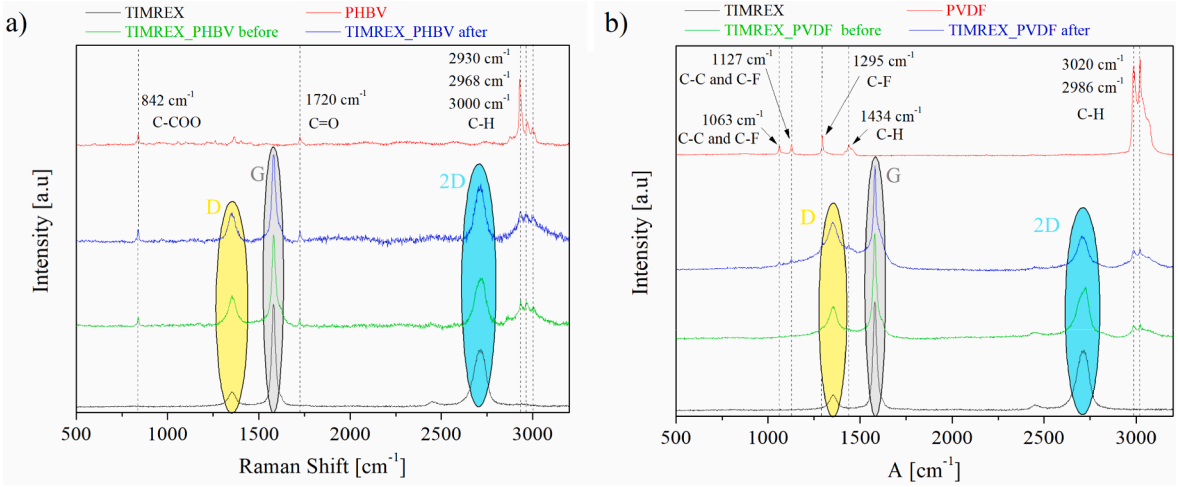

Fig. 6. Raman spectra of electrode material with PHBV (a) and PVDF (b) as a binder before and after electrochemical measurements.

caused by the fact that PHBV was first dissolved for electrode fabrication while the Raman spectrum of PHBV was done for solid material. Nevertheless, the presence of signals coming from PHBV in TIMREX_PHBV after electrochemical tests suggests that PHBV was still present in the electrode material. The Raman measurements confirmed the stability of the PHBV binder under electrochemical treatment.

In the case of TIMREX_PVDF electrode material, the presence of PVDF is confirmed by the peaks located at 1063 cm^{-1}, 1127 cm^{-1}, 1295 cm^{-1} and 1434 cm^{-1}. These bands are attributed to C—F and C—C bonds in the polymer matrix, whereas signals at 2986 cm^{-1} and 3020 cm^{-1} confirm the presence of C—H bond in the methylene group [39].

To investigate the influence of the binder type on the charge transfer processes, galvanostatic intermittent titration technique (GITT) was applied. This technique allows for determining the diffusion coefficient of lithium ions (D_{Li^+}), the value of which is strongly affected by the stoichiometry of the host. To calculate the D_{Li^+} value, the formula given by Aurbach *et al.* was used [40]:

$$D = \frac{4 \cdot l^2}{\pi \cdot \Delta t_p} \left(\frac{\Delta E_s}{\Delta E_t} \right)^2 \quad \text{at } t << \tau \tag{6}$$

where l is diffusion length (the film thickness), Δt_p – time of the galvanostatic pulse duration, ΔE_s – the change of a steady-state (equilibrium) voltage at the end of two sequential open-circuit relaxation periods, ΔE_t – the total change in the cell voltage during the current pulse, τ – refers to short time approximation.

In the case of $t \ll \tau$ one can be sure that the semi-infinite diffusion of lithium ions takes place in the bulk of the electrode material. The values of D_{Li^+}, calculated from Equation (6), for TIMREX_PHBV and TIMREX_PVDF electrode materials are plotted in Fig. 7a and 7b, respectively. The regions at which the current maxima for the studied electrode materials were identified, are presented in Fig. 2c. The shape of the curve shown in the insets in Fig. 7a and 7b is affected by the different stoichiometry of the intercalated graphene layers. This phenomenon refers to different intercalation mechanisms at different potential values, as was previously observed for the graphite electrode [19]. The more lithium ions are intercalated into graphene layers, the lower D_{Li^+} values are observed. The curves obtained for both TIMREX_PHBV and TIMREX_PVDF electrode materials look rather similar. Regardless of the binder type used, the obtained values of apparent diffusion coefficient are of the same order of magnitude. Thus, it may be concluded that the replacement of PVDF with PHBV does not affect the charge transfer process of lithium ions into the graphite electrode.

4. Conclusions

The results presented in this paper consistently demonstrate the feasibility of using green materials for producing components for Li-ion batteries.

The PHBV-based electrode material was successfully prepared by

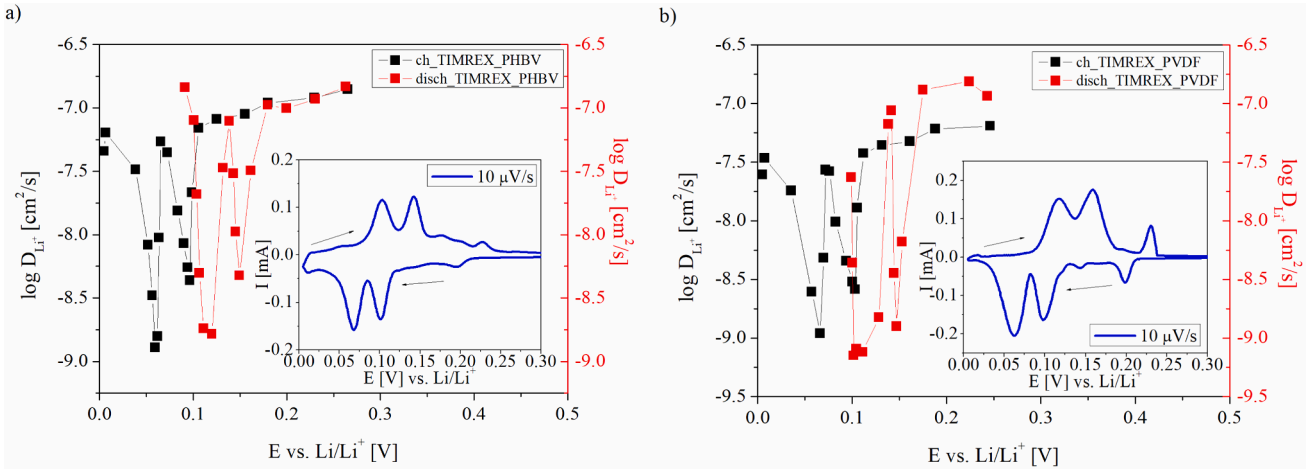

Fig. 7. Plots of the chemical diffusion coefficient (log D) as a function of the electrode potential for graphite electrode materials with a) PHBV binder and b) PVDF binder analysed by GITT. Insets: the cv curve of the investigated anode materials at $v = 10$ μV/s.

MOST WIEDZY Downloaded from mostwiedzy.pl

direct mixing of graphite, PHBV and carbon black. It was shown that PHBV exhibits a similar bonding ability as the conventional PVDF binder, namely the negative electrodes consisting of these binders were presenting very similar electrochemical performance, including both the shape of the cv curves and specific capacities. The capacity retention for PHBV binder after 100 cycles at 36 mA/g was 99.1 % and capacity reached 357 mAh/g. Furthermore, the diffusion coefficient of lithium ions within both PHBV and PVDF electrode materials was of the same order of magnitude, and changed in the range from 10^{-9} to 10^{-7} [cm^2/s]. Moreover, no significant differences in morphology were observed for the PHBV-based electrode material before and after galvanostatic charge/discharge tests. The Raman measurements prove that there is no degradation of PHBV during long-term electrode polarization. It evidences that PHBV might replace PVDF as a binder in negative electrode for LIBs, as both electrode materials exhibits similar electrochemical performance.

CRediT authorship contribution statement

Andrzej P. Nowak: Conceptualization, Methodology, Investigation, Resources, Writing – original draft, Supervision, Project administration. **Konrad Trzciński:** Investigation, Writing – original draft. **Zuzanna Zarach:** Visualization, Writing – original draft, Writing – review & editing. **Jinjin Li:** Resources, Writing – review & editing. **Daria Roda:** Investigation, Visualization, Writing – review & editing. **Mariusz Szkoda:** Investigation, Resources, Writing – review & editing, Funding acquisition.

Declaration of Competing Interest

The authors declare the following financial interests/personal relationships which may be considered as potential competing interests: Szkoda Mariusz reports financial support was provided by National Centre for Research and Development.

Data availability

Data will be made available on request.

Acknowledgements

This work is financially supported by The National Centre for Research and Development via grant no LIDER/15/0088/L-10/18/NCBR/2019 (Integrated prototype of a photosupercapacitor for energy storage obtained as a result of solar radiation conversion) and from BEETHOVEN CLASSIC 3 program of The National Science Centre (Project “Beyond Li-ion batteries: On novel and Efficient electrode materials for Sodium Storage,” Grant no. UMO-2018/31/G/ST5/02056).

Appendix A. Supplementary material

Supplementary data to this article can be found online at https://doi.org/10.1016/j.apsusc.2022.154933.

References

[1] H. An, X. Li, C. Chalker, M. Stracke, R. Verduzco, J.L. Lutkenhaus, Conducting Block Copolymer Binders for Carbon-Free Hybrid Vanadium Pentoxide Cathodes with Enhanced Performance, ACS Appl. Mater. Interfaces 8 (2016) 28585–28591.
[2] J. Landesfeind, A. Eldiven, H.A. Gasteiger, Influence of the Binder on Lithium Ion Battery Electrode Tortuosity and Performance, J. Electrochem. Soc. 165 (2018) A1122–A1128.
[3] A. Cholewinski, P. Si, M. Uceda, M. Pope, B. Zhao, Polymer binders: Characterization and development toward aqueous electrode fabrication for sustainability, Polymers (Basel). 13 (2021) 1–20.
[4] V.H. Nguyen, W.L. Wang, E.M. Jin, H.B. Gu, Impacts of different polymer binders on electrochemical properties of LiFePO4 cathode, Appl. Surf. Sci. 282 (2013) 444–449.
[5] T.C. Nirmale, B.B. Kale, A.J. Varma, A review on cellulose and lignin based binders and electrodes: Small steps towards a sustainable lithium ion battery, Int. J. Biol. Macromol. 103 (2017) 1032–1043.
[6] X. Zhong, J. Han, L. Chen, W. Liu, F. Jiao, H. Zhu, W. Qin, Binding mechanisms of PVDF in lithium ion batteries, Appl. Surf. Sci. 553 (2021).
[7] V. Ponnuchamy, E.S. Esakkimuthu, Density functional theory study of lignin, carboxymethylcellulose and unsustainable binders with graphene for electrodes in lithium-ion batteries, Appl. Surf. Sci. 573 (2022) 151461.
[8] A.P. Nowak, K. Trzciński, M. Szkoda, G. Trykowski, M. Gazda, J. Karczewski, M. Łapiński, D. Maskowicz, M. Sawczak, A. Lisowska-Oleksiak, Nano Tin/Tin Oxide Attached onto Graphene Oxide Skeleton as a Fluorine Free Anode Material for Lithium-Ion Batteries, Inorg. Chem. 59 (2020) 4150–4159.
[9] R. Wang, L. Feng, W. Yang, Y. Zhang, Y. Zhang, W. Bai, B. Liu, W. Zhang, Y. Chuan, Z. Zheng, et al., Effect of Different Binders on the Electrochemical Performance of Metal Oxide Anode for Lithium-Ion Batteries, Nanoscale Res. Lett. 12 (2017).
[10] G. Kang dong, Y. Cao, ming Application and modification of poly(vinylidene fluoride) (PVDF) membranes - A review, J. Memb. Sci. 463 (2014) 145–165.
[11] Solvay Solef® PVDF for Li-Ion Batteries Available online: https://www.solvay.com/en/brands/solef-pvdf/li-ion-batteries.
[12] W.B. Hawley, A. Parejiya, Y. Bai, H.M. Meyer, D.L. Wood, J. Li, Lithium and transition metal dissolution due to aqueous processing in lithium-ion battery cathode active materials, J. Power Sources 466 (2020) 228315.
[13] A.D. Pasquier, F. Disma, T. Bowmer, A.S. Gozdz, G. Amatucci, J.-M. Tarascon, Differential Scanning Calorimetry Study of the Reactivity of Carbon Anodes in Plastic Li-Ion Batteries, J. Electrochem. Soc. 145 (1998) 472–477.
[14] J. Li, J. Fleetwood, W.B. Hawley, W. Kays, From Materials to Cell: State-of-the-Art and Prospective Technologies for Lithium-Ion Battery Electrode Processing, Chem. Rev. 122 (2022) 903–956.
[15] D.L. Wood, J.D. Quass, J. Li, S. Ahmed, D. Ventola, C. Daniel, Technical and economic analysis of solvent-based lithium-ion electrode drying with water and NMP, Dry. Technol. 36 (2018) 234–244.
[16] M. Mancini, F. Nobili, R. Tossici, M. Wohlfahrt-Mehrens, R. Marassi, High performance, environmentally friendly and low cost anodes for lithium-ion battery based on TiO2 anatase and water soluble binder carboxymethyl cellulose, J. Power Sources 196 (2011) 9665–9671.
[17] H. Buqa, M. Holzapfel, F. Krumeich, C. Veit, P. Novák, Study of styrene butadiene rubber and sodium methyl cellulose as binder for negative electrodes in lithium-ion batteries, J. Power Sources 161 (2006) 617–622.
[18] S.H. Joo, Y. Liang, M. Kim, J. Byun, H. Choi, Microplastics with adsorbed contaminants: Mechanisms and Treatment, Environ. Challenges 3 (2021) 100042.
[19] G. Keskin, G. Klzll, M. Bechelany, C. Pochat-Bohatier, M. Öner, Potential of polyhydroxyalkanoate (PHA) polymers family as substitutes of petroleum based polymers for packaging applications and solutions brought by their composites to form barrier materials, Pure Appl. Chem. 89 (2017) 1841–1848.
[20] A. Balakrishna Pillai, A. Jaya Kumar, H. Kumarapillai, Biosynthesis of poly(3-hydroxybutyrate-co-3-hydroxyvalerate) (PHBV) in Bacillus aryabhattai and cytotoxicity evaluation of PHBV/poly(ethylene glycol) blends, 3 Biotech 10 (2020) 1–10.
[21] J. Liu, Y. Zhao, M. Diao, W. Wang, W. Hua, S. Wu, P. Chen, R. Ruan, Y. Cheng, Poly (3-hydroxybutyrate-co-3-hydroxyvalerate) Production by Rhodospirillum rubrum Using a Two-Step Culture Strategy, J. Chem. 2019 (2019.).
[22] M.I. Ibrahim, D. Alsafadi, K.A. Alamry, M.A. Hussein, Properties and Applications of Poly(3-hydroxybutyrate-co-3-hydroxyvalerate) Biocomposites, J. Polym. Environ. 29 (2021) 1010–1030.
[23] J. Mergaert, C. Anderson, A. Wouters, J. Swings, K. Kersters, Biodegradation of polyhydroxyalkanoates, FEMS Microbiol. Lett. 103 (1992) 317–321.
[24] S.K. Heiskanen, J. Kim, B.L. Lucht, Generation and Evolution of the Solid Electrolyte Interphase of Lithium-Ion Batteries, Joule 3 (2019) 2322–2333.
[25] S.A. Barenberg, J.L. Brash, R. Narayan, A.E. Redpath, Degradable Materials Perspectives, Issues, and Opportunities, CRC Press, 2018, ISBN 9781315892221.
[26] M. Biron, Future prospects for thermoplastics and thermoplastic composites, in Thermoplastics and Thermoplastic Composites, Elsevier B.V, 2007, pp. 829-861 ISBN 9781856174787.
[27] M.D. Levi, D. Aurbach, The mechanism of lithium intercalation in graphite film electrodes in aprotic media. Part 1. High resolution slow scan rate cyclic voltammetric studies and modeling, J. Electroanal. Chem. 421 (1997) 79–88.
[28] T. Ohzuku, Y. Iwakoshi, K. Sawai, Formation of Lithium-Graphite Intercalation Compounds in Nonaqueous Electrolytes and Their Application as a Negative Electrode for a Lithium Ion (Shuttlecock) Cell, J. Electrochem. Soc. 140 (1993) 2490–2498.
[29] S. Lee, Molecular Dynamics Study of the Separation Behavior at the Interface between PVDF Binder and Copper Current Collector, J. Nanomater. 2016 (2016).
[30] X. Zhong, J. Han, L. Chen, W. Liu, F. Jiao, H. Zhu, W. Qin, Binding mechanisms of PVDF in lithium ion batteries, Appl. Surf. Sci. 553 (2021) 149564.
[31] N. Cuesta, A. Ramos, I. Cameán, C. Antuña, A.B. García, Hydrocolloids as binders for graphite anodes of lithium-ion batteries, Electrochim. Acta 155 (2015) 140–147.
[32] E. Peled, S. Menkin, Review—SEI: Past, Present and Future, J. Electrochem. Soc. 164 (2017) A1703–A1719.
[33] A. Berrueta, I. San Martín, P. Sanchis, A. Ursúa, Lithium-ion batteries as distributed energy storage systems for microgrids, 2019, ISBN 9780128177747.
[34] T.J. Shaffner, R.D. Van Veld, “Charging” effects in the scanning electron microscope, J. Phys. E. 4 (1971) 633–637.
[35] A. Sadezky, H. Muckenhuber, H. Grothe, R. Niessner, U. Pöschl, Raman microspectroscopy of soot and related carbonaceous materials: Spectral analysis and structural information, Carbon N. Y. 43 (2005) 1731–1742.

MOST WIEDZY Downloaded from mostwiedzy.pl

[36] A.P. Nowak, K. Trzciński, M. Szkoda, J. Karczewski, M. Gazda, A. Lisowska-Oleksiak, A negative effect of carbon phase on specific capacity of electrode material consisted of nanosized bismuth vanadate embedded in carbonaceous matrix, Synth. Met. 257 (2019).
[37] J. Wu Bin, M.L. Lin, X. Cong, H.N. Liu, P.H. Tan, Raman spectroscopy of graphene-based materials and its applications in related devices, Chem. Soc. Rev. 47 (2018) 1822–1873.
[38] C.M.S. Izumi, M.L.A. Temperini, FT-Raman investigation of biodegradable polymers: Poly(3-hydroxybutyrate) and poly(3-hydroxybutyrate-co-3-hydroxyvalerate), Vib. Spectrosc. 54 (2010) 127–132.
[39] D. Chipara, V. Kuncser, K. Lozano, M. Alcoutlabi, E. Ibrahim, M. Chipara, Spectroscopic investigations on PVDF-Fe2O3 nanocomposites, J. Appl. Polym. Sci. 137 (2020) 1–13.
[40] M.D. Levi, K. Gamolsky, D. Aurbach, U. Heider, R. Oesten, Determination of the Li ion chemical diffusion coefficient for the topotactic solid-state reactions occurring via a two-phase or single-phase solid solution pathway, J. Electroanal. Chem. 477 (1999) 32–40.

MOST WIEDZY Downloaded from mostwiedzy.pl